AGU PUBLICATIONS

JGR

Journal of Geophysical Research: Oceans

RESEARCH ARTICLE
10.1002/2014JC009874

Special Section:
Pacific-Asian Marginal Seas

Key Points:
- Primary productivity was two times higher in the EJS than in the WSP
- Primary production in the UB was enhanced by large phytoplankton
- Vertical water column structure determines phytoplankton dynamics

Correspondence to:
C.-K. Kang,
ckkang@gist.ac.kr

Citation:
Kwak, J. H., S. H. Lee, J. Hwang, Y.-S. Suh, H. J. Park, K.-I. Chang, K.-R. Kim, and C.-K. Kang (2014), Summer primary productivity and phytoplankton community composition driven by different hydrographic structures in the East/Japan Sea and the Western Subarctic Pacific, *J. Geophys. Res. Oceans*, *119*, 4505–4519, doi:10.1002/2014JC009874.

Received 30 JAN 2014
Accepted 28 JUN 2014
Accepted article online 2 JUL 2014
Published online 23 JUL 2014

Summer primary productivity and phytoplankton community composition driven by different hydrographic structures in the East/Japan Sea and the Western Subarctic Pacific

Jung Hyun Kwak[1], Sang Heon Lee[2], Jeomshik Hwang[3], Young-Sang Suh[4], Hyun Je Park[1], Kyung-Il Chang[3], Kyung-Ryul Kim[3], and Chang-Keun Kang[1]

[1]School of Environmental Science and Engineering, Gwangju Institute of Science and Technology, Gwangju, South Korea, [2]Department of Oceanography, Pusan National University, Busan, South Korea, [3]School of Earth and Environmental Sciences, Seoul National University, Seoul, South Korea, [4]National Fisheries Research and Development Institute, Busan, South Korea

Abstract The East/Japan Sea (EJS) is a highly productive marginal sea in the northwest Pacific, consisting of three basins (Ulleung Basin: UB, Yamato Basin: YB, and Japan Basin: JB). To find causes of the reportedly high primary productivity in summer in the EJS, especially in the UB, we measured primary productivity, phytoplankton composition, and other environmental variables. The water column was strongly stratified in the EJS compared with the Western Subarctic Pacific (WSP). Integrated primary productivity was two times higher in the EJS (612 mg C m^{-2} d^{-1}) than in the WSP (291 mg C m^{-2} d^{-1}). The vertical distributions of physicochemical and biological factors confirmed that production in the subsurface chlorophyll maximum layer in the study regions was an important factor regulating primary productivity within the water column. While picoplankton ($<$2.7 μm) dominated in the WSP, JB, and YB, micro/nanoplankton ($\geq$2.7 μm) dominated in the UB. Contribution by picoplankton to total biomass and primary productivity in the UB was significantly lower than in the other regions. CHEMTAX analysis using marker pigments showed that diverse phytoplankton groups inhabited the study regions. Cluster and canonical correspondence analyses showed high correlation between the spatial variation in phytoplankton assemblages with the water mass properties mainly represented by water temperature and nitrate concentration. Overall, our results suggest that the hydrographic structure of water column in the study region is an important controlling factor of the biomass and productivity of phytoplankton as well as their diversity in size and taxonomic groups.

1. Introduction

The East/Japan Sea (EJS) is one of the highly productive oceanic regions in the temperate zone [*Yamada et al.*, 2005; *Ashjian et al.*, 2006; *Lee et al.*, 2009]. The EJS with an area of 1.01 $\times$ 10^6 km^2 is a semienclosed marginal sea connected to the northwestern Pacific Ocean through narrow and shallow straits (i.e., Korea/Tsushima, Tsugaru, Soya, and Tatar Straits). It contains three deep ($>$2000 m) basins (Figure 1): the Ulleung Basin (UB), the Yamato Basin (YB), and the Japan Basin (JB). Hydrographic features of the EJS (e.g., deep water formation, independent thermohaline circulation, a subpolar front, and mesoscale eddies) are similar to those of the North Atlantic Ocean [*Min and Warner*, 2005; *Riser and Jacobs*, 2005; *Talley et al.*, 2006]. Because of these ocean-like features, the EJS is considered to be an ideal place for studying oceanic processes as a "Miniature Ocean" [*Kim and Kim*, 1996; *Lee et al.*, 2009]. The EJS is experiencing notable environmental changes (i.e., variation of water mass structure and the climate regime shift), also accompanying changes in community structure and ecosystem processes [*Kim and Kim*, 1996; *Kim et al.*, 2001; *Rebstock and Kang*, 2003; *Kang et al.*, 2004; *Zhang and Gong*, 2005; *Lee et al.*, 2009; *Gong and Suh*, 2012].

The UB, located in the southwestern part of the EJS, is reportedly the most productive region among the three deep basins in the EJS based on satellite observations [*Yamada et al.*, 2005]. A few hypotheses have been suggested as the main cause of the high primary productivity in the UB. These include physical processes such as coastal upwelling and mesoscale eddies [*Hyun et al.*, 2009; *Yoo and Park*, 2009; *Kim et al.*, 2012; *Lim et al.*, 2012]. A recent study that compared summer primary productivity in the UB with that in the subtropical western Pacific and the East China Sea suggested that the relatively high rates of primary

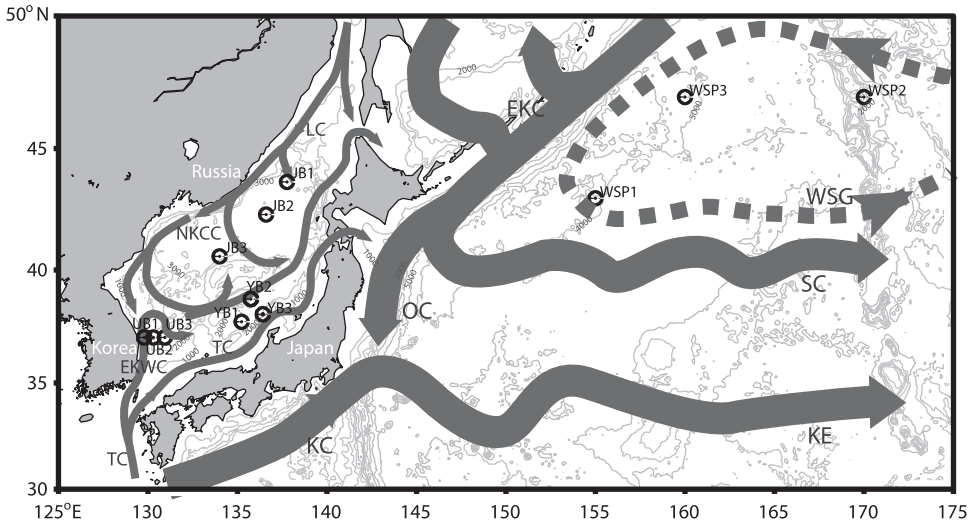

Figure 1. Overview of study region with sampling locations and currents from June to July 2010 in the Ulleung Basin, the Yamato Basin, the Japan Basin, and the Western Subarctic Pacific. Key: UB-1-3, Ulleung Basin; YB-1-3, Yamato Basin; JB-1-3, Japan Basin; and WSP-1-3, Western Subarctic Pacific; KC, Kuroshio Current; KE, Kuroshio Current Extension; EKC, East Kamchatka Current; OC, Oyashio Current; SC, Subarctic Current; WSG, Western Subarctic Gyre; LC, Liman Current; NKCC, North Korean Cold Current; EKWC, East Korean Warm Current; and TWC, Tsushima Warm Current.

productivity in the UB is supported by increased nitrate (NO_3) supply from nutrient-rich deeper waters to the euphotic zone because of the shallow pycnocline in summer [*Kwak et al*., 2013a]. *Kwak et al*. [2013a] also suggested that high summer primary productivity in the UB may be attributed to the production in the SCM layer.

However, primary productivity is expected to be controlled by various physicochemical and biological factors. For example, the vertical position of the SCM layer in relation to light and nutrient availability can control phytoplankton biomass and productivity [*Martin et al*., 2010]. *Kwak et al*. [2013b] observed that the generation and destruction of the SCM layer and the associated shift in phytoplankton assemblages are related to the nature of the water column structure in the UB. Phytoplankton size and community composition directly reflect the response of phytoplankton assemblages to environmental variations [*Margalef*, 1978; *Malone*, 1980; *Elser et al*., 1986; *Piontkovski et al*., 1995; *Iriarte et al*., 2000]. Therefore, hydrographic conditions and biological features such as plankton size and community composition and vertical location of SCM will influence primary production complicatedly. However, there are few studies dealing with these factors in relation to hydrographic properties, especially in the EJS where primary productivity is considerably higher than the surrounding open waters [*Lee et al*., 2009].

In this study, we attempted to understand the role of hydrographic conditions such as stratification in summer to biology represented by phytoplankton size distribution and community composition and ultimately to water column-integrated primary productivity. We mainly compare the EJS with the Western Subarctic Pacific (WSP) for this purpose although there is about a month gap between the two measurements. The WSP is also characterized by enhanced primary productivity supported by nutrient supply as a terminal zone of the deep water circulation [*Koblents-Mishke et al*., 1970; *Honda et al*., 2002]. SCM is also observed in the WSP, although the intensity is weaker than in the EJS.

2. Materials and Methods

2.1. Sample Collection

Samples were collected during three cruises in summer 2010 in the EJS and in the WSP aboard the R/Vs Hakuho Maru and Eardo (Figure 1). Two cruises were in the WSP, the JB, and the YB in 21 June 2010 to 23 July 2010 (KH-10-02, legs 2 and 3) and the other cruise was in the UB in 19 July 2010 to 1 August 2010. We selected three representative stations in each region (i.e., stations UB-1 through 3, YB-1 through 3, JB-1 through 3, and WSP-1 through 3). Water samples were collected between the surface and 200 m depth

using a CTD-rosette system equipped with 10 L Niskin bottles. The samples for carbon uptake rate determination were collected at five or six optical depths corresponding to 100, (50), 30, 15, 5, and 1% light penetration based on Secchi disk depth measurements [*Poole and Atkins*, 1929]. Water samples for nutrient and pigment analysis were collected at the same depths, and additional standard depths of 75, 100, 150, and 200 m.

2.2. Hydrography and Nutrients

Temperature, salinity, and depth were obtained with a CTD (SBE 911 Plus, Seabird Electronics Inc., Bellevue, WA, USA). The lower boundary of the surface mixed layer was determined by a density increase of 0.125 σ_t from the surface value [*Gardner et al*., 1995]. The stability index was defined as the ratio of the difference in σ_t between the surface and the 50 m depth to the thickness of the euphotic zone [*Cho et al*., 2001]. Water samples for nutrient analysis were filtered through Whatman GF/F filters. The filtered seawater samples were immediately transferred into acid-washed polyethylene bottles and frozen at −20°C. In the land-based laboratory, nitrate (NO_3), phosphate (PO_4), and silicate (SiO_4) were measured by standard spectrophotometric methods [*Parsons et al*., 1984].

2.3. Carbon Uptake Rate Determination

Samples were prefiltered through 200 μm mesh Nytex net and dispensed into two sets of 0.5 L transparent polycarbonate Nalgene bottles. Light intensity was measured on board using a photosynthetically available radiation sensor (Li-1400, Li-cor Inc., Lincoln, NE, USA) to determine the daily and experimental irradiance. For determination of the carbon uptake rate, $NaH^{13}CO_3$ (98 at. %, Isotec, Sigma-Aldrich, St Louis, OH, USA) solution was spiked to each sample used for incubation to a final concentration of 0.2 mM, corresponding to about 10% of the ambient concentration. The bottles were covered with calibrated number of layers of screens to mimic the irradiance equivalent to those at five or six optical depths. The water samples were then incubated on deck under natural light for 3–4 h in two acrylic incubators. Incubation temperature was controlled by irrigation with surface seawater for the samples from the upper two or three depths and by a cooling system for the samples from the lower three depths. At the end of the incubation, the water samples were filtered through precombusted (at 450°C for 2 h) 25 mm Whatman GF/D and GF/F filters under gentle vacuum, and the filters were stored at −20°C until isotopic analysis.

The particle samples for POC concentration and ^{13}C isotope ratio measurements were fumed with HCl for 12 h to remove carbonate and then dried at 60°C. The treated samples were analyzed with a carbon-hydrogen-nitrogen elemental analyzer (3000 Series, Eurovector, Milan, Italy) coupled with a continuous-flow isotope ratio mass spectrometer (IsoPrime, GV Instruments, Manchester, UK). Carbon uptake rate was estimated following *Hama et al*. [1983]. Specific primary productivity is defined as a chlorophyll *a*-specific carbon uptake rate (mg C m^{-3} d^{-1} (mg Chl)$^{-1}$). Daily primary productivity (mg C m^{-3} d^{-1}) was calculated by multiplying the measured hourly carbon uptake rate with photoperiod conversion factors [*Kanda et al*., 1985; *Fan and Glibert*, 2005]. Integrated primary productivity (mg C m^{-2} d^{-1}) was calculated using the trapezoidal rule for the entire euphotic zone (1–100% of surface irradiance).

2.4. Pigment and Chemotaxonomic Analysis on Size-Fractionated Samples

Water samples for pigment analysis were filtered gently through 47 mm Whatman GF/D and GF/F filters (nominal pore sizes 2.7 and 0.7 μm, respectively). The filters were wrapped in aluminum foil and kept frozen (−80°C) until analysis using high-performance liquid chromatography (Shimadzu Co., Kyoto, Japan). The samples for pigment analysis were extracted with 5 mL of 95% methanol for 12 h in the dark at −20°C and sonicated for 10 min. The extracted solution was centrifuged to remove cellular and glass filter debris and then supernatant was filtered through a 0.45 μm PTFE syringe filter. An aliquot of the filtered solution was mixed with 300 μL of water and then 100 μL of this solution was analyzed by reverse-phase HPLC equipped with a Waters Symmetry C_8 column (4.6 × 150 mm; particle size 3.5 μm; 100 Å pore size), using a method modified from *Zapata et al*. [2000]. The pure standard pigments, obtained from Sigma-Aldrich (St. Louis, MO, USA) and DHI (Hamburg, Germany), were used for identification. Quantification of standard pigments was done using known specific extinction coefficients [*Jeffrey*, 1997].

Based on pigment composition and concentrations, phytoplankton community composition was estimated from the ratio of each biomarker pigment to chlorophyll *a*, using CHEMTAX software [*Mackey et al*., 1996;

Wright and van den Enden, 2000]. Twelve diagnostic biomarker pigments—chlorophyll *a*, fucoxanthin, 19′-hexanoyloxy-fucoxanthin, 19′-butanoyloxy-fucoxanthin, neoxanthin, peridinin, chlorophyll *b*, prasinoxanthin, lutein, violaxanthin, alloxanthin, and zeaxanthin—were used. Class-specific pigment ratios determined from various species collected around the Korean peninsula [*Lee et al*., 2011] were used as the input pigment ratios of the CHEMTAX program. Cluster analysis of phytoplankton assemblage was applied to each station and depth, and any dissimilarity between stations and depths was calculated using a Bray-Curtis similarity matrix. Canonical correspondence analysis (CCA) is the technique selected for the best linear combination of environmental variables that maximize the dispersion of the species scores [*Braak and Verdouschot*, 1995]. CCA using the CANOCO program was adopted to outline relationships between environmental factors, phytoplankton group, and phytoplankton assemblage at each station and depth [*Braak*, 1986; *Sundbäck and Snoeijis*, 1991]. Integrated values of pigment concentrations were calculated using the by trapezoidal integration from surface to 100 m.

One-way ANOVA was used to make spatial comparisons of primary productivity and pigment concentrations, and subsequent pair-wise comparisons were conducted with Tukey's HSD (honestly significant differences) test. Student's *t* test was performed to test differences in micro and nanosized chlorophyll *a* concentrations between warm and cold-water masses. Because almost all the data did not significantly deviate from a normal distribution (Shapiro-Wilk test, $p < 0.05$), no prior transformation of the data was performed. Only fucoxanthin concentrations were logarithmically transformed to meet the assumption of a normal distribution. Homogeneity was checked using the Levene test. A commercially available software package was used to test spatial differences of productivity and pigment variables (SPSS, package, Chicago, IL).

3. Results

3.1. Hydrography and Nutrients

Sea surface temperatures were notably higher in the EJS (17.7–24.8°C) than in the WSP (5.8–12.9°C) even at similar latitudes. The water column was strongly stratified in the EJS, but not in the WSP (Figure 2). Density in the EJS increased abruptly from the surface to 50 m depth and very slowly below this depth. Accordingly, the surface mixed layer depth was much shallower in the EJS than in the WSP (Table 1). A steep thermocline within about 20 m was the major cause of the strong stratification in the JB and the YB. In comparison, in the UB, relatively low salinity in the surface layer along with a vertical temperature gradient caused strong stratification of the water column. Overall, the surface mixed layer was thin in the EJS and the stability index in the EJS was five times higher than in the WSP (Table 1).

NO_3, SiO_4, and PO_4 all showed similar vertical profiles (Figure 3). NO_3 concentrations in the surface layer were relatively low in the EJS (0.1−0.2 μM) compared to those in the WSP (0.3−3.9 μM). The low NO_3 concentrations were accompanied by a gradual increase below the surface mixed layer with maximum values exceeding 4 μM at 75 m in the EJS, but by a sharp increase beneath the surface (0 m) in the WSP. The SiO_4 and PO_4 concentrations in the surface layer were low (0.2−4.0 and 0.0−0.4 μM, respectively) in the study regions and increased up to 3.6−20.7 and 0.6−3.5 μM in the EJS and to 17.9−41.4 and 1.0−1.9 μM, respectively, in the WSP within 75 m of depth.

3.2. Chlorophyll, Primary Production, and Phytoplankton Size Distribution

Chlorophyll *a* concentrations were generally low in the surface (0.2 mg m^{-3}), tending to increase in the upper water column (10–50 m) and then to decrease with increasing depth (Figure 4). The concentrations in the SCM were slightly higher (one-way ANOVA, $p = 0.009$; Tukey's test, $p = 0.05$) in the YB and the UB (0.4–0.9 mg m^{-3}) than in the WSP and the JB (0.2–0.4 mg m^{-3}). Integrated chlorophyll *a* concentration from surface to 100 m was also higher (one-way ANOVA, $p = 0.005$; Tukey's test, $p = 0.05$) in the YB and the UB (mean ± SD, 36 ± 8 and 26 ± 6 mg m^{-2}, respectively) than in the JB and the WSP (16 ± 3 and 19 ± 2 mg m^{-2}, respectively).

Vertical profiles of primary productivity were different from the distributions of chlorophyll *a* concentration (Figure 5). The maximum primary productivity (10–24 mg C m^{-3} d^{-1}) in the WSP was observed in the surface layer (0–10 m), whereas the maximum primary productivity (13–29 mg C m^{-3} d^{-1}) in the EJS was observed in the subsurface layer (10–20 m) except for Station YB-1, where the highest POC concentration

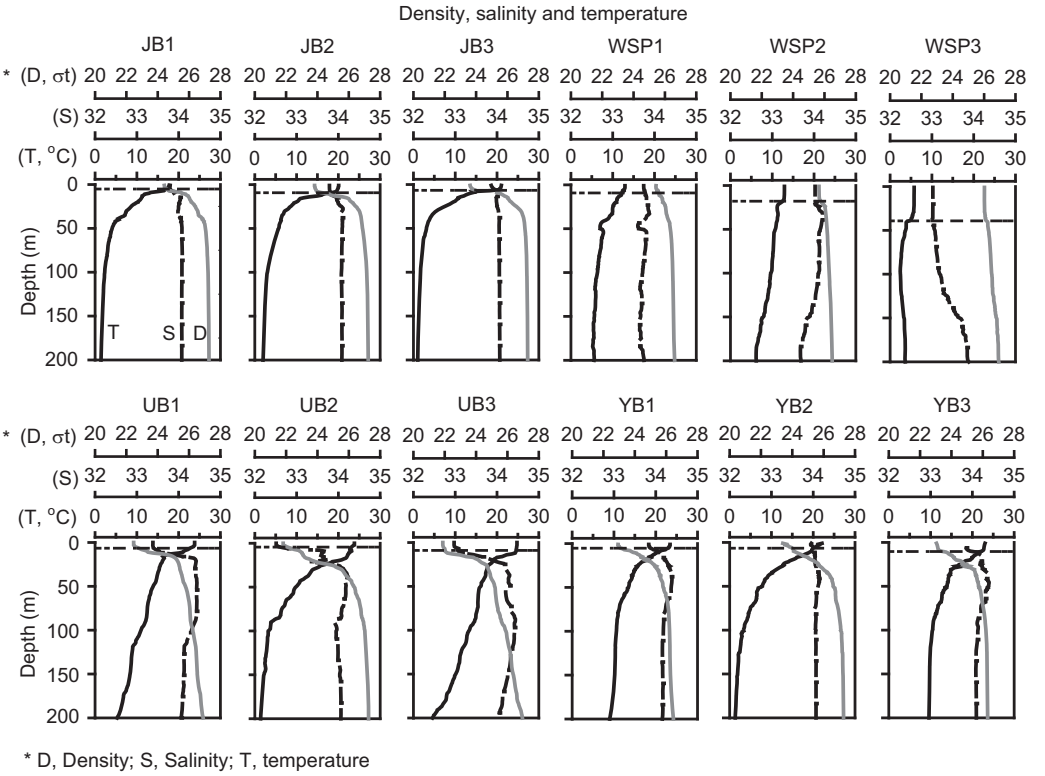

Figure 2. Vertical profiles of density (σ_t), temperature, and salinity at stations located in the JB, WSP, UB, and YB. Horizontal dashed lines represent the surface mixed layer.

and carbon-to-chlorophyll ratio among all sampling stations were observed (data not shown). Integrated primary productivity ranged from 260 (Station WSP-3) to 760 mg C m^{-2} d^{-1} (Station UB-1). While no significant difference in the maximum primary productivity was found between the WSP and the EJS (one-way ANOVA, $p = 0.398$), the average integrated primary productivity (610 mg C m^{-2} d^{-1}) in the EJS was about two times than that in the WSP (290 mg C m^{-2} d^{-1}). Specific primary productivity ranged from 4 (at 5% light penetration depth at Station YB-1) to 180 mg C m^{-3} d^{-1} (mg Chl)$^{-1}$ (at the surface at Station YB-1; Figure 6). The vertical variation of specific primary productivity was similar to that of primary productivity (Figures 5 and 6). The vertically averaged specific primary productivity was also 1.5 times in the EJS than in the WSP (Table 1).

During the study period, the biomass and primary production contributions of micro/nanoplankton in the UB were higher than that of picoplankton, whereas the contribution of picoplankton was higher than micro/nanoplankton in other locations (Table 1). Also, in the case of integrated primary production, contributions of picoplankton (64–92%) was higher (one-way ANOVA, $p < 0.001$; Tukey's test, $p = 0.01$) than those

Table 1. Mixed Layer Depth, Euphotic Depth, Stability Index, Integrated Values of Chlorophyll a and Primary Productivity, and Depth-Average of Specific Primary Productivity in the Study Regions

					Chlorophyll *a*		Integrated Primary Productivity (IPP)		
Region	Date	Ranges of Latitude and Longitude	Mixed Layer Depth (m)	Stability Index	Integrated Chl *a* (mg m^{-2})	Contribution of Picoplankton (%)	IPP (mg C m^{-2} d^{-1})	Contribution of Picoplankton (%)	Specific Primary Productivity [mg C m^{-3} d^{-1} (mg Chl)$^{-1}$]
WSP	23–29 Jun	43.0°N–47.0°N, 155.0°E–170.0°E	22 ± 16	1.2 ± 0.7	16 ± 3	63 ± 5	291 ± 34	69 ± 5	37 ± 34
JB	5–11 Jul	40.4°N–43.4°N, 134.0°E–137.5°E	6 ± 2	6.1 ± 0.9	19 ± 2	56 ± 5	526 ± 102	85 ± 5	55 ± 41
YB	18–20 Jul	37.5°N–38.5°N, 135.1°E–136.3°E	6 ± 3	4.3 ± 0.4	36 ± 8	56 ± 10	594 ± 120	82 ± 9	57 ± 52
UB	22–24 Jul	37.0°N–37.0°N, 129.5°E–130.6°E	6 ± 2	7.4 ± 0.8	26 ± 6	38 ± 16	716 ± 42	35 ± 2	61 ± 25

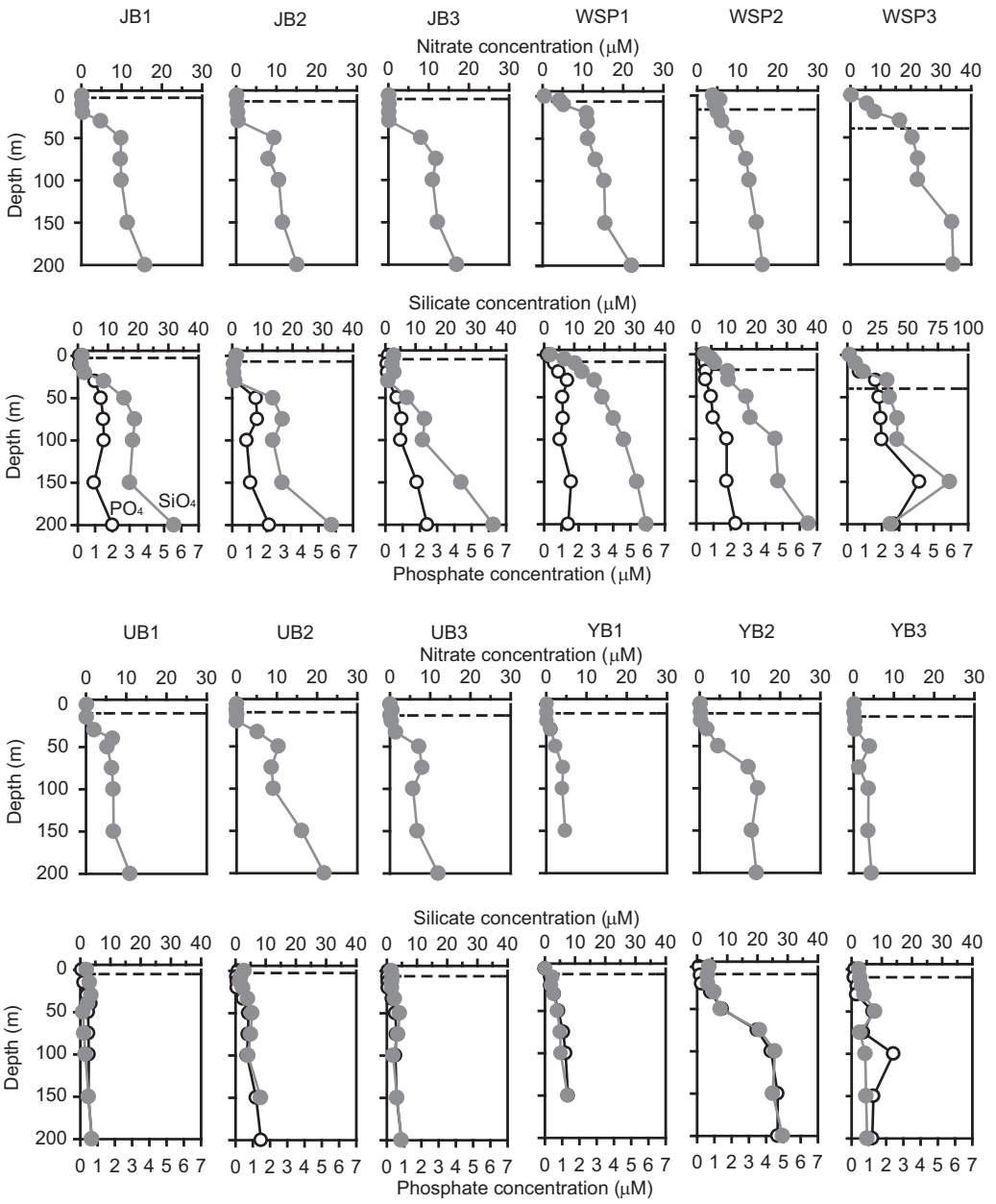

Figure 3. Vertical profiles of NO_3, SiO_4, and PO_4 at stations located in the JB, WSP, UB, and YB. Horizontal dashed lines represent the surface mixed layer.

of the micro/nanoplankton in the WSP, the JB, and the YB (Table 1), whereas picoplankton contributed 34–38% of the integrated primary productivity in the UB.

3.3. Pigment and CHEMTAX Analysis

All pigment classes analyzed were generally undetectable below 75 m and hence pigment data for the upper 75 m layer are presented. The distribution of diagnostic pigments was quite variable among stations, showing various patterns without any predominance of a particular pigment class. Concentrations of neoxanthin, violaxanthin, alloxanthin, and lutein were negligible (<37 ng L^{-1}) throughout the upper 75 m layer. In the WSP, vertical distributions of fucoxanthin, a marker pigment of diatoms, resembled those of chlorophyll *a*, but the concentrations were relatively low (<76 ng L^{-1}). At Station WSP-1, samples of prasinophythin and chlorophyll *b*, a marker pigment of picosized green algae including prasinophytes, resembled

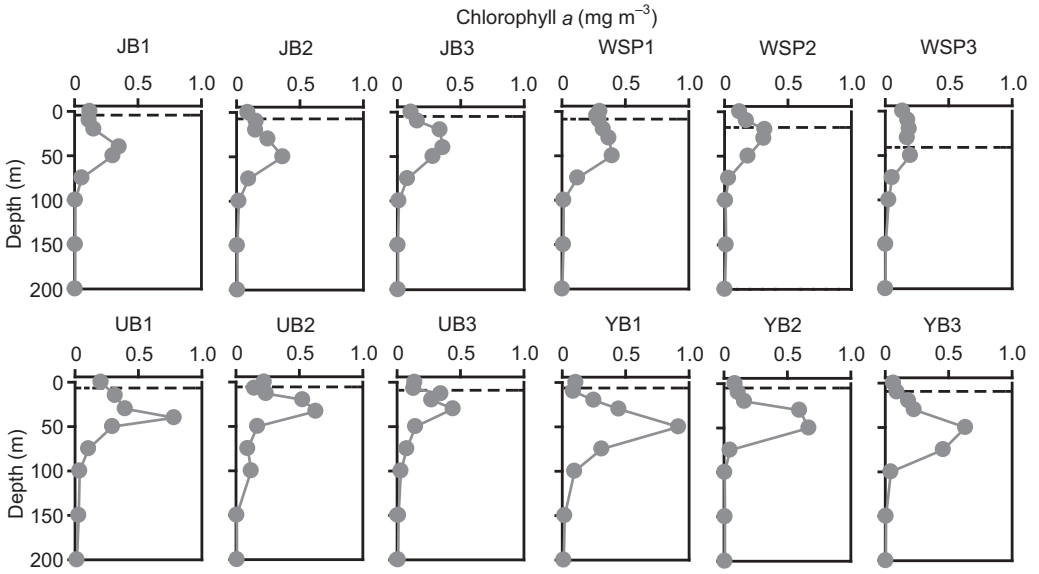

Figure 4. Vertical profiles of chlorophyll *a* concentration at stations located in the JB, WSP, UB, and YB. Horizontal dashed lines represent the surface mixed layer.

those of chlorophyll *a*, and concentrations of these pigments in the SCM increased up to 110 and 230 ng L^{-1}, respectively. At Station WSP-2, the distributional pattern of 19′-butanoyloxy-fucoxanthin, a marker pigment of prymnesiophytes, was similar to that of chlorophyll *a*, and the concentration increased up to 190 ng L^{-1} in the SCM layer. In the EJS, the distributions of fucoxanthin, 19′-butanoloxy-fucoxanthin, 19′-hexanoyloxy-fucoxanthin, peridinin, and chlorophyll *b* were similar to those of chlorophyll *a*, but concentrations of these classes differed among stations. Concentrations of fucoxanthin in the SCM were higher (one-way ANOVA, $p = 0.027$; Tukey's test, $p = 0.05$) in the EJS (100–1600 ng L^{-1}) than were those in the WSP (39–67 ng L^{-1}). The highest concentration of fucoxanthin was found in the SCM layer at Station UB-1. Concentrations of zeaxanthin, a marker pigment of cyanobacteria, were generally low (<40 ng L^{-1}). Vertical distributions of zeaxanthin concentration differed from those of chlorophyll *a*, and maximal zeaxanthin concentrations were found in the surface layer or over the SCM layer. Concentrations of 19′-hexanoyloxy-fucoxanthin, a marker

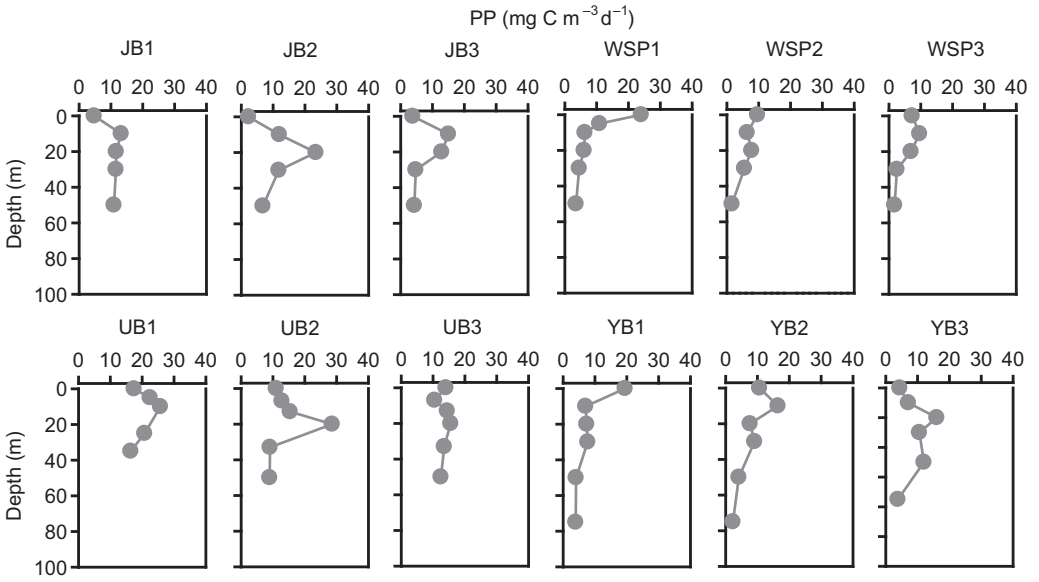

Figure 5. Vertical profiles of primary productivity (PP) at stations located in the JB, WSP, UB, and YB.

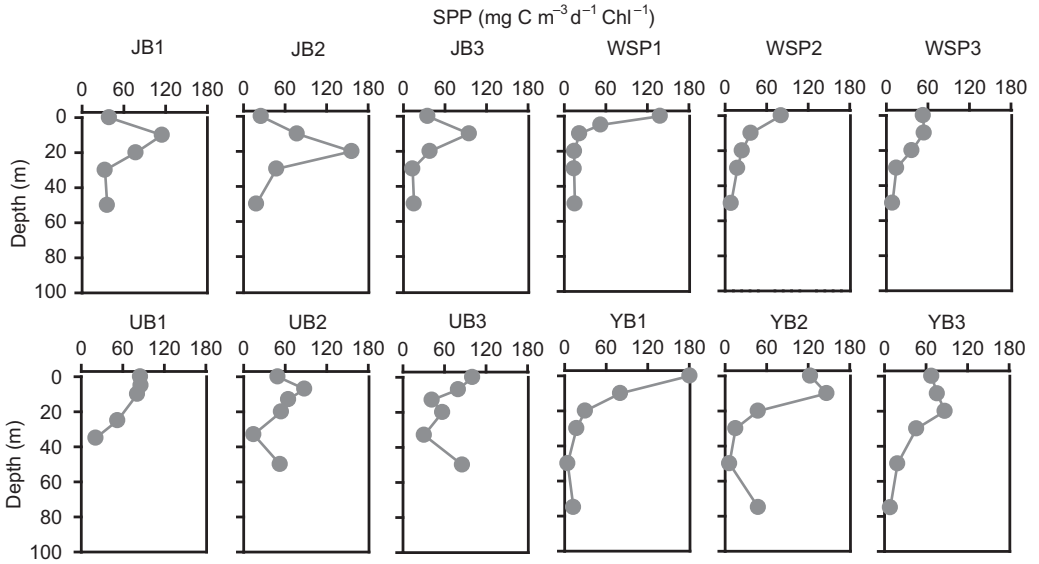

Figure 6. Vertical profiles of specific primary productivity (SPP) at stations located in the JB, WSP, UB, and YB.

pigment of pelagophytes and prymnesiophytes, ranged from 14 to 190 ng L^{-1} in the SCM in the WSP and 64 to 550 ng L^{-1} in the EJS. Concentrations of peridinin, a marker pigment of dinoflagellates, were generally low (<35 ng L^{-1}), but increased up to 5400 and 210 ng L^{-1} at Stations UB-1 and UB-3, respectively.

CHEMTAX analysis from pigment data revealed the distributions of the various phytoplankton taxa and the phytoplankton community compositions. The relative contributions of phytoplankton groups indicated that no specific phytoplankton groups were dominant (>40%) except for at Station YB-1 where prymnesiophytes accounted for over 70% of the total chlorophyll *a* concentration (Figure 7a). The contribution of each phytoplankton group to chlorophyll *a* varied widely in both picosized and micro and nanosized fractions (Figures 7b and 7c). However, the contributions of picosized chlorophytes and cyanobacteria were generally low (<4.4 and 7.6%, respectively). Integrated chlorophyll *a* concentrations of micro/nanoplankton were higher (Student's *t* test, $p = 0.006$) in the warm water masses (i.e., the UB and the YB, 9.5–24 mg m^{-2}) than in the cold-water masses (i.e., the JB and the WSP, 5.8–9.3 mg m^{-2}).

Phytoplankton taxa based on the chemosynthetic taxonomic analysis were divided into nine clusters at the 55% level of a Bray-Curtis similarity index (Figure 8). With a few exceptions, almost all the samples were clustered into five groups (A–E). Group A consisted of phytoplankton assemblages in the upper euphotic layer in the EJS, and Group B consisted of assemblages at the depth of 75 m in every region. Groups C, D, and E were affiliated with the other assemblages showing complicated compositions at different stations and depths.

4. Discussion

4.1. Influence of Hydrographic Conditions on Primary Productivity

One of the most notable hydrographic features was the strong water column stratification in the EJS, but only weak one in the WSP (Figure 1). While high temperature and/or low salinity in the surface in the EJS induced the stable water column structure, low surface water temperature in the WSP (6−13°C) caused a relatively deeper mixed layer depth and consequently, lower stability (Table 1). Vertical variation of chlorophyll *a* concentration and primary productivity may be mainly related to the different hydrographic structures in each region. In the EJS, relatively low primary productivity in the surface mixed layer is caused by the strong stratification and consequent limitation in nutrient supply (Figures 1, 3, and 5). NO_3 appears to be a major limiting factor for primary productivity in surface water in the EJS. Recently, *Kwak et al.* [2013a] suggested that high summer primary productivity in the UB was supported by NO_3 supply from deeper

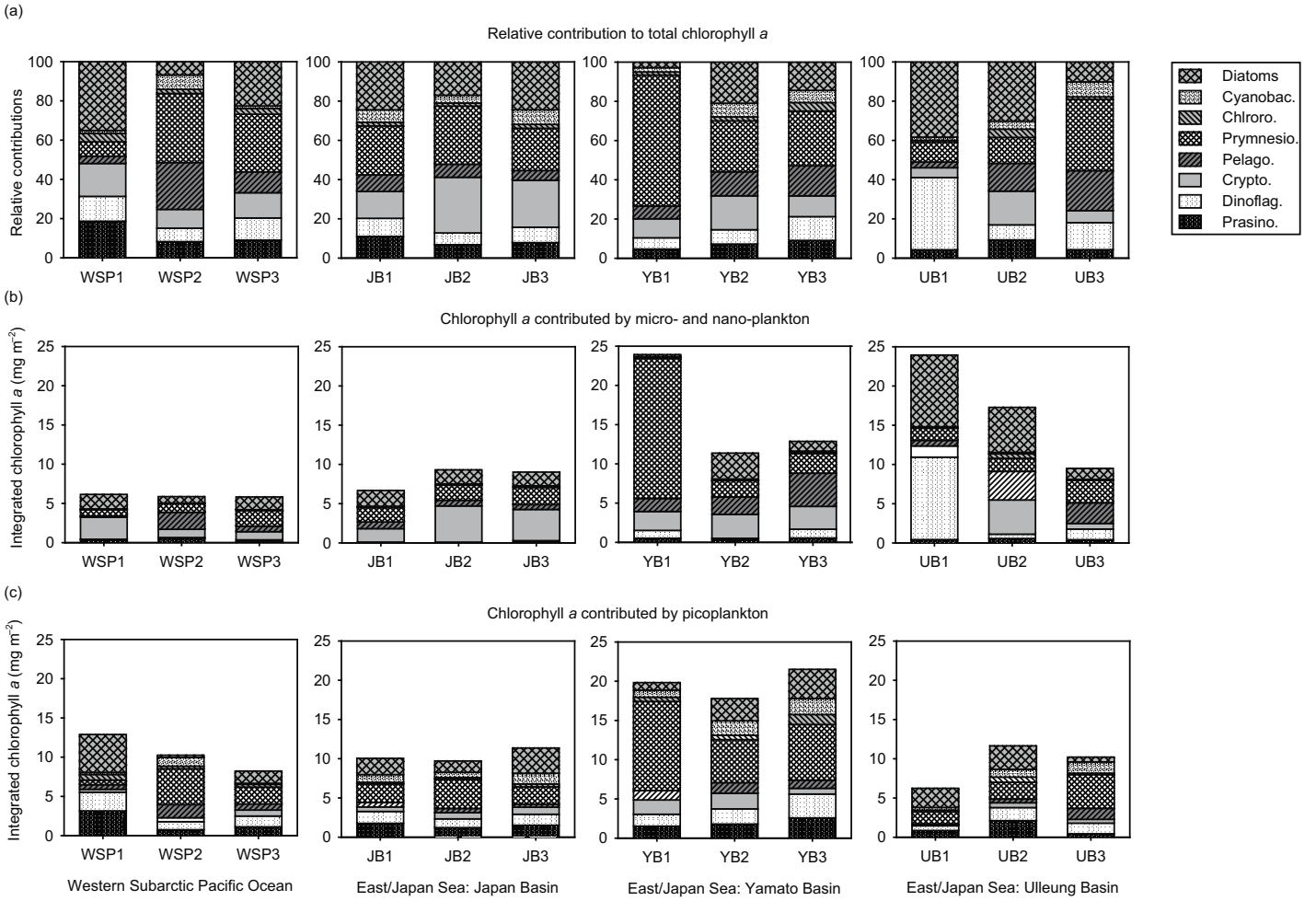

Figure 7. (a) Relative contributions of phytoplankton groups to total phytoplankton biomass, (b) contributions of phytoplankton groups to microsized and nanosized plankton, and (c) picoplankton at stations located in the WSP, JB, YB, and UB. Key: Cyanobac., cyanobacteria; Chloro., chlorophytes; Prymnesio., prymnesiophytes; Pelago., pelagophytes; Crypto., cryptophytes; Dinoflag., dinoflagellates; and Prasino., prasinophytes.

water in the summer. The maximum rates of primary productivity in the EJS were generally observed in the upper nitracline (Figures 3 and 5) further demonstrating the importance of NO_3 availability in controlling primary productivity in the EJS. In contrast, in the WSP, the maximum primary productivity was observed in the surface layer (0–10 m deep), representing better supply of nutrients from nutrient-rich deeper water to the surface.

Although nutrient concentrations in the euphotic zone (<75 m) were higher in the WSP than in the EJS, the integrated primary productivity was higher in the EJS than in the WSP [*Shiomoto*, 2000; *Yamada et al*., 2005; *Kwak et al*., 2013a, 2013b]. In the WSP, calculated integrated summer primary productivity (291 $\pm$ 34 mg C m^{-2} d^{-1}) was similar to the value estimated by *Shiomoto* [2000] (247 $\pm$ 177 mg C m^{-2} d^{-1}) and by *Honda et al*. [2002] (220 mg C m^{-2} d^{-1} at Station KNOT in the WSP from May 1998 to December 1999). The weak stratification leading to deep mixing in the WSP produced stressful conditions for phytoplankton growth by reducing the available light energy and forcing buoyancy, thereby inhibiting phytoplankton growth [*Lozier et al*., 2011]. Iron limitation may be another cause as suggested by *Nishioka et al*. [2003] and *Harrison et al*. [2004].

The SCM layer is an important factor influencing phytoplankton biomass and productivity in offshore regions [*Cullen*, 1982; *Lee and Whitledge*, 2005]. The SCM layer is generally observed during stratification periods in the western North Pacific Ocean including the EJS [*Furuya and Marumo*, 1983; *Rho et al*., 2012]. Chlorophyll *a* concentrations in the SCM layer contributed a large portion (up to 87.5%) of depth-integrated

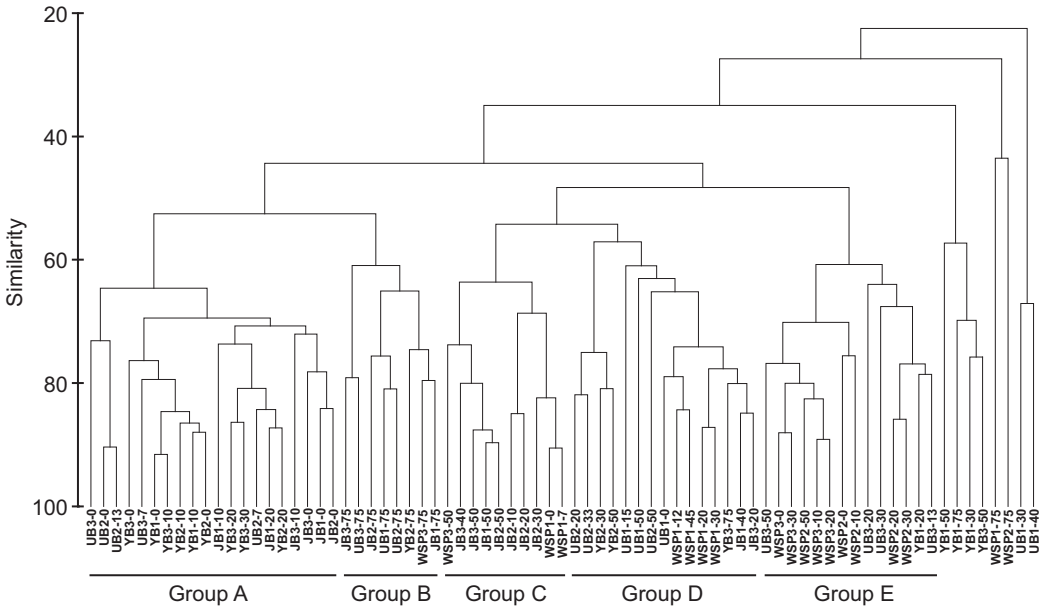

Figure 8. Groups clustered by the Bray-Curtis index based on phytoplankton abundance and assemblage at station/depth combinations located in the JB, WSP, UB, and YB.

chlorophyll *a* concentration in the UB [*Kwak et al*., 2013b]. Although no strict relationship between chlorophyll *a* concentration and primary productivity was observed in the present study, primary productivity in the SCM layer in the EJS contributed to a large portion of the total primary productivity at least partly because of its thickness (Figure 4). At the stations in the EJS where primary productivity was maximized in the subsurface, the highest specific rates of primary productivity were observed there rather than in the surface, with the exception of Station UB-1 (Figures 5 and 6). This station is located at the slope break near the east coast of the Korean peninsula; hence, horizontal supply of nutrients from the coastal upwelling was plausible [*Yoo and Park*, 2009].

A negative role of the SCM to production in the surface mixed layer is hindrance of vertical nutrient supply. The relatively low specific primary productivity in the surface in the EJS suggests that nutrient limitation here may have been caused by high rate of NO_3 uptake in the subsurface layers. Thus, exhaustion of NO_3 by phytoplankton in the SCM layer appears to limit the surface primary productivity, although the supply of NO_3 from nutrient-rich deeper water enhanced summer primary productivity in the SCM layer. Overall effect of the production in the SCM layer to the water column-integrated primary productivity should be examined more carefully.

4.2. Size-Fractionated Chlorophyll *a* and Primary Productivity

While nutrient concentrations were higher in the cold water (the JB and the WSP) than in the warm water (the UB and the YB), total phytoplankton biomass was higher in the UB and YB than in the JB and the WSP. The concentration of micro/nanoplankton and their contribution to total phytoplankton biomass was also higher in the UB and at Station YB-1 than in the JB and the WSP. Another interesting feature is that although chlorophyll *a* concentration was higher in the YB than in the UB, primary productivity was higher in the UB than in the YB. We attempt to explain the causes of these features considering the size distribution of phytoplankton, grazing by zooplankton, and the location of the SCM layer.

One potential control of the spatial phytoplankton size distribution is grazing by zooplankton. In the WSP, large copepods occupy the epipelagic zone in summer [*Kobari and Ikeda*, 1999; *Mackas and Tsuda*, 1999], but in the EJS, zooplankton species compositions are distinguished by different water mass types of cold northern and warm southern regions [*Meshcheryakova*, 1960]. *Ashjian et al*. [2005] found that the northern EJS was mainly inhabited by large colder-water species (i.e., large copepods) and the southern EJS was dominated by small warmer water species (i.e., small copepods). The vertical distribution of zooplankton composition was also associated with water temperature; that is, large copepods migrate downward to

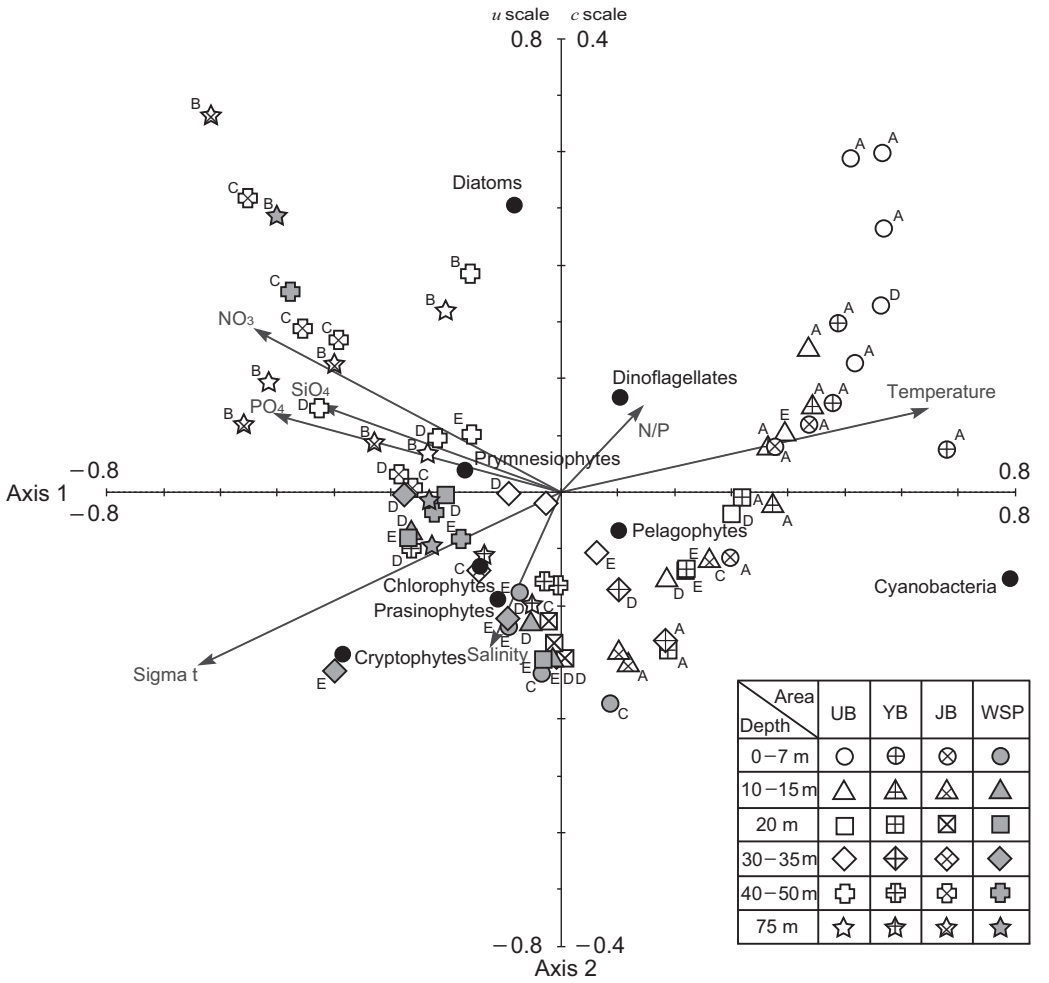

Figure 9. Ordination diagram obtained from canonical correspondence analysis based on phytoplankton abundance and assemblage at station/depth combinations located in the JB, WSP, UB, and YB with respect to phytoplankton groups and environmental factors.

colder (<10°C) water while small copepods migrate upward to warmer (>12°C) water [*Ashjian et al*., 2006]. With respect to their food selectivity, large copepods feed preferentially on large phytoplankton (i.e., diatoms), whereas small copepods feed randomly or preferably on prymnesiophytes [*Head and Harris*, 1994]. *Jansen* [2008] observed that small copepods did not feed on large diatom species. In this respect, the strikingly high phytoplankton biomass observed at Station YB-1, where a high concentration of prymnesiophytes and high water temperature (>10°C) were observed in the euphotic zone, might have arisen from low grazing pressure (Figures 2 and 7). Several studies have reported that phytoplankton size composition and biomass are controlled by zooplankton grazing [*Malone and Chervin*, 1979; *Burkill et al*., 1995; *Han and Furuya*, 2000; *Chiba and Saino*, 2002; *Yamamura et al*., 2002]. *Hiromi* [1996] also found that grazing by zooplankton heavily depressed the phytoplankton biomass and productivity in Tokyo Bay. These findings suggest that the zooplankton species composition and their selective feeding habits may have been an important factor in determining the phytoplankton cell size and biomass in the study region.

Fluctuations of phytoplankton size composition and in their physiological status can affect primary productivity and photosynthetic efficiency [*Han and Furuya*, 2000]. Primary productivity was higher in the UB than in the YB, although chlorophyll *a* concentration was higher in the YB than in the UB (Figure 4 and Table 1). This somewhat unexpected observation might have resulted from the high contribution of large phytoplankton to integrated phytoplankton biomass and productivity in the UB compared with that in the other regions. The contribution of small phytoplankton to total biomass and integrated primary productivity was slightly lower in the YB than in the UB regions during the study period, reflecting a low specific primary

Table 2. Summary of the Results From Canonical Correspondence Analysis (CCA)

	Axes 1	Axes 2	Axes 3	Axes 4	Total Inertia
Eigenvalues	0.010	0.003	0.001	0.001	0.051
Species-environment correlations	0.812	0.490	0.440	0.428	
Cumulative percentage variance of species data	19.1	25.8	28.7	30.9	
Cumulative percentage variance of species-environment relation	59.5	80.7	89.6	96.6	
Sum of all unconstrained eigenvalues					0.051
Sum of all canonical eigenvalues					0.016

	Canonical Coefficients		Inter Set Correlations	
	Axes 1	Axes 2	Axes 1	Axes 2
NO_3	2.5292	−3.4029	−0.6289	0.1304
DIN	−3.2330	5.3913	−0.6250	0.1198
NH_4	0.3931	−1.1769	−0.2657	−0.0569
SiO_4	0.3601	−1.1140	−0.4860	0.0688
PO_4	−0.1690	−0.0651	−0.5838	0.0618
Temperature	0.7005	−4.8588	0.7543	0.0658
Salinity	−0.1128	1.3215	−0.1380	−0.1181
Sigma *t*	−0.0097	−5.6319	−0.7467	−0.1395
NP ratio	0.0768	−0.1360	0.1542	0.0629

productivity. From a study in the Chukchi Sea, *Lee et al*. [2013] suggested that the increase in the contribution of small phytoplankton to total biomass could decrease total primary production and that the specific primary productivities of small phytoplankton were significantly lower than those of large ones.

Martin et al. [2010] suggested that shoaling of the SCM layer could enhance integrated primary productivity because of an increase in light availability. The shallower SCM depth in the UB (30–40 m) compared with that in the YB (50 m) was also an important factor for increasing specific primary productivity. Overall, the relatively high rates of primary productivity in the UB mainly resulted from the high contribution of large phytoplankton to biomass and productivity with a shallower SCM depth compared with the YB (Figure 4).

4.3. Hydrographic Properties and Phytoplankton Community Structure

Phytoplankton assemblages deduced from marker pigments varied widely both vertically and horizontally (Figures 7 and 8). The assemblages were classified into five major groups (Figure 8). Group A and B assemblages ($<$0.25 and 0.10 mg m^{-3}, respectively) appear to be associated with low Chlorophyll *a* concentration, being mostly located in the upper euphotic layer in the EJS and near the bottom of the euphotic layer. While the main components of Group A in the EJS were cyanobacteria and diatoms, those of Group B were prymnesiophytes and diatoms. The major phytoplankton taxa in Groups C, D, and E were cryptophytes, diatoms, and prymnesiophytes, respectively.

Phytoplankton physiological state, photosynthetic efficiency, and adaptation to environmental variables are known to affect phytoplankton community structures [*Krupatkina*, 1991; *Piontkovski et al*., 1995]. Therefore, it is not feasible to explain the spatial variation in phytoplankton assemblage by one particular environmental variable in the study region. To further understand the relative contribution of environmental variables in controlling the phytoplankton community structure, we performed a canonical correspondence analysis. The canonical correspondence analysis revealed the relationships between environmental factors and phytoplankton taxa (Figure 9 and Table 2). The CCA showed that the ordination diagram for the first two axes (axes 1 and 2) covered about 81% of the variance in phytoplankton taxa with respect to environmental factors (note that in Figure 9, the *c* scale of the triplot on the basis of the CCA applies to environmental variables, and the *u* scale to phytoplankton taxa and stations and depths).

Expectedly, the arrow representing the water temperature variable has significantly negative correlation with sigma t and nutrients reflecting the vertical variation in water column properties. The other factors show relatively low correlations (short arrow lengths) with phytoplankton taxa. The symbols representing each station-depth combination were scattered on the triplot revealing the high spatial variation of phytoplankton community composition. Cyanobacteria are located in the far right of the plot showing a positive correlation with temperature, and negative ones with nutrients. The position of the cryptophytes is in the

far left of the plot. The other taxa are located near zero on the axis 1 and more dispersed on the triplot, reflecting the influences of multiple factors other than water temperature and nutrients.

Highly variable environmental conditions caused by strong stratification of the water column can lead to unique phytoplankton assemblages vertically separated at a given station. The phytoplankton assemblage in the shallow (≤20 m deep) surface layer of the EJS was closely associated with high temperature and oligotrophic conditions, displaying a dominance of cyanobacteria, pelagophytes, and small dinoflagellates and diatoms. In contrast, the assemblage in the deeper layer in the EJS (also at deeper euphotic depth of the WSP) reflected low temperatures and eutrophic conditions below the surface mixed layer, consisting mainly of large diatoms and prymnesiophytes. The major components of phytoplankton assemblages in the surface and subsurface layer in the WSP, where a cold and nutrient-rich water mass prevailed, were prymnesiophytes, diatoms, chlorophytes, and prasinophytes. Therefore, horizontally and vertically different environmental conditions appear to allow phytoplankton to be very diverse in this study region.

5. Summary

The water column structure in summer was characterized by strong stratification in the EJS compared with the WSP. Integrated primary productivity in the EJS was higher than that in the WSP during the study period despite the more favorable nutrient concentrations in the WSP. This high productivity in the EJS is believed to result from the maximal subsurface productivity in the upper SCM layer. However, the strong stratification and exhaustion of nutrients within the SCM layer leads to nutrient limitation in the surface mixed layer, causing a relatively low primary productivity in the surface layer in the EJS. The biomass of large phytoplankton was greater in the warm water masses (the UB and YB) than in the cold-water masses (the JB and the WSP). In addition, the high contribution of large phytoplankton to total biomass and primary productivity with high water column-averaged specific primary productivity was mainly responsible for the relatively high integrated primary productivity in the UB compared with that in the YB in the EJS.

Phytoplankton composition and biomass were regulated by water column stability, nutrient supply, and zooplankton grazing in the study region. Overall, our results suggest that: (1) the EJS and the WSP are occupied by diverse phytoplankton groups, without any single dominant species in summer and (2) the observed diversity in phytoplankton assemblage is caused by different characteristics of water column.

Acknowledgments
We would like to thank the captains and crews of R/Vs Hakuho Maru and Eardo. We are also grateful to J. Zhang and K. Imai for help with sampling. This research was carried out as a part of "East Asian Seas Time series-I (EAST-I)" funded by the Ministry of Oceans and Fisheries, Korea, and "Monitoring of Harmful Algal Bloom and Study on the Occurrence and Mechanism (RP-2014-ME-006)" funded by the National Fisheries Research and Development Institute, Korea.

References

Ashjian, C. J., C. S. Davis, S. M. Gallager, and P. Alatalo (2005), Characterization of the zooplankton community, size composition, and distribution in relation to hydrography in the Japan/East Sea, *Deep Sea Res., Part II*, *52*, 1363–1392.
Ashjian, C. J., R. Arnone, C. S. Davis, B. Jones, M. Kahru, C. Lee, and G. Mitchell (2006), Biological structure and seasonality in the Japan/East Sea, *Oceanography*, *19*, 122–133.
Braak, C. J. F. (1986), Canonical correspondence analysis: A new eigenvector technique for multivariate direct gradient analysis, *Ecology*, *67*, 1167–1179.
Braak, C. J. F., and P. F. M. Verdonschot (1995), Canonical correspondence analysis and related multivariate methods in aquatic ecology, *Aquat. Sci.*, *57*, 1015–1621.
Burkill, P. H., E. S. Edwards, and M. A. Sleigh (1995), Microzooplankton and their role in controlling phytoplankton growth in the marginal ice zone of the Bellingshausen Sea, *Deep Sea Res., Part II*, *42*, 1277–1290.
Chiba, S., and T. Saino (2002), Interdecadal change in the upper water column environment and spring diatom community structure in the Japan Sea: An early summer hypothesis, *Mar. Ecol. Prog. Ser.*, *231*, 23–35.
Cho, B. C., M. G. Park, J. H. Shim, and D. H. Choi (2001), Sea-surface temperature and *f*-ratio explain large variability in the ratio of bacterial production to primary production in the Yellow Sea, *Mar. Ecol. Prog. Ser.*, *216*, 31–41.
Cullen, J. J. (1982), The deep chlorophyll maximum: Comparing vertical profiles of chlorophyll *a*, *Can. J. Fish. Aquat. Sci.*, *39*, 791–803.
Elser, J. J., M. M. Elser, and S. R. Carpenter (1986), Size fraction of algal chlorophyll, carbon fixation and phosphatase activity: Relationships with species-specific size distributions and zooplankton community structure, *J. Plankton Res.*, *8*, 365–383.
Fan, C., and P. M. Glibert (2005), Effects of light on nitrogen and carbon uptake during a *Prorocentrum minimum* bloom, *Harmful Algae*, *4*, 629–641.
Furuya, K., and R. Marumo (1983), The structure of the phytoplankton community in the subsurface chlorophyll maxima in the western North Pacific Ocean, *J. Plankton Res.*, *5*, 393–406.
Gardner, W. D., S. P. Chung, M. J. Richardson, and I. D. Walsh (1995), The oceanic mixed- layer pump, *Deep Sea Res.*, Part II, *42*, 757–775.
Gong, Y., and Y. S. Suh (2012), Climate change and fluctuations of populations in the Far East region, *J. Ecol. Field Biol.*, *35*, 15–25.
Hama, T., T. Miyazaki, Y. Ogawa, M. Iwakuma, M. Takahashi, A. Otsuki, and S. Ichimura (1983), Measurement of photosynthetic production of a marine phytoplankton population using a stable isotop 13C isotope, *Mar. Biol.*, *73*, 31–36.
Han, M.-S., and K. Furuya (2000), Size and species-specific primary productivity and community structure of phytoplankton in Tokyo Bay, *J. Plankton Res.*, *22*, 1221–1235.
Harrison, P. J., F. A. Whitney, A. Tsuda, and H. Saito (2004), Nutrient and plankton dynamics in the NE and NW Gyres of the Subarctic Pacific Ocean, *J. Oceanogr.*, *60*, 93–117.

Head, E. J. H., and L. R. Harris (1994), Feeding selectivity by copepods grazing on natural mixtures of phytoplankton determined by HPLC analysis of pigments, *Mar. Ecol. Prog. Ser.*, *110*, 75–83.
Hiromi, J. (1996), Potential impact of grazing by *Oithona davisae* (Copepoda, Cyclopoida) in Tokyo Bay, summer, *Bull. Coll. Agric. Veterinary Medicine Nihon Univ.*, *53*, 47–55.
Honda, M. C., K. Imai, Y. Nojiri, F. Hoshi, T. Sugawara, and M. Kusakabe (2002), The biological pump in the northwestern North Pacific based on fluxes and major components of particulate matter obtained by sediment-trap experiments (1997–2000), *Deep Sea Res., Part II*, *49*, 5595–5625.
Hyun, J. H., D. Kim, C. W. Shin, J. H. Noh, E. J. Yang, J. S. Mok, S. H. Kim, H. C. Kim, and S. Yoo (2009), Enhanced phytoplankton and bacterioplankton production coupled to coastal upwelling and an anticyclonic eddy in the Ulleung Basin, East Sea, *Aquat. Microbial Ecol.*, *54*, 45–54.
Iriarte, J. L., G. Pizarro, V. A. Troncoso, and M. Sobarzo (2000), Primary production and biomass of size-fractionated phytoplankton off Antofagasta, Chile (23−24°S) during pre-El Niño and El Niño 1997, *J. Mar. Syst.*, *26*, 37–51.
Jansen, S. (2008), Copepods grazing on *Coscinodiscus wailesii:* A question of size?, *Helgol. Mar. Res.*, 62, 251–255.
Jeffrey, S. W. (1997), Application of pigment methods to oceanography, in *Phytoplankton Pigments in Oceanography: Guidelines to Modern Methods*, edited by S. W. Jeffery, R. F. C. Mantoura, and S. W. Wright, pp. 127–166, UNESCO Publ., Paris.
Kanda, J., T. Saino, and A. Hattori (1985), Nitrogen uptake by natural populations of phytoplankton and primary production in the Pacific Ocean: Regional variability of uptake capacity, *Limnol. Oceanogr.*, *30*, 987–999.
Kang, D.-J., K. Kim, and K.-R. Kim (2004), The past, present and future of the East/Japan Sea in change: A simple moving-boundary box model approach, *Prog. Oceanogr.*, *61*, 175–191.
Kim, D., E. J. Yang, K. H. Kim, C.-W. Shin, J. Park, S. Yoo, and J.-H. Hyun (2012), Impact of an anticyclonic eddy on the summer nutrient and chlorophyll a distributions in the Ulleung Basin, East Sea (Japan Sea), *ICES J. Mar. Sci.*, *69*, 23–29.
Kim, K., K.-R. Kim, D.-H. Min, Y. Volkov, J.-H. Yoon, and M. Takemaatsu (2001), Warming and structure changes in the East (Japan) Sea: A clue to future changes in global oceans?, *Geophys. Res. Lett.*, *28*, 3293–3296.
Kim, K.-R., and K. Kim (1996), What is happening in the East Sea (Japan Sea)? Recent chemical observations from CREAMS 93−96, *J. Korean Soc. Oceanogr.*, *31*, 164–172.
Kobari, K., and T. Ikeda (1999), Vertical distribution, population structure and life cycle of *Neocalanus cristatus* (Crustacea: Copepoda) in the Oyashio region, with notes on its regional variations, *Mar. Biol.*, *134*, 683–696.
Koblents-Mishke, O. I., V. V. Volkovinsky, and Yu. G. Kabanova (1970), Plankton primary production of the world ocean, in *Scientific Exploration of the South Pacific*, edited by W. Wooster, pp. 183–193, Natl. Acad. of Sci., Washington, D. C.
Krupatkina, D. K. (1991), Primary production and size-fractionated structure of the Black Sea phytoplankton in the winter-spring period, *Mar. Ecol. Prog. Ser.*, *73*, 25–31.
Kwak, J. H., J. Hwang, E. J. Choy, H. J. Park, D.-J. Kang, T. Lee, K.-I. Chang, K.-R. Kim, and C. K. Kang (2013a), High primary productivity and f-ratio in summer in the Ulleung Basin of the East/Japan Sea, *Deep Sea Res., Part I*, *79*, 74–85.
Kwak, J. H., S. H. Lee, H. J. Park, E. J. Choy, H. D. Jeong, K. R. Kim, and C. K. Kang (2013b), Monthly measured primary and new productivities in the Ulleung Basin as a biological "hot spot" in the East/Japan Sea, *Biogeosciences*, *10*, 4405–4417.
Lee, J. Y., D. J. Kang, I. N. Kim, T. Rho, T. Lee, C. K. Kang, and K. R. Kim (2009), Spatial and temporal variability in the pelagic ecosystem of the East Sea (Sea of Japan): A review, *J. Mar. Syst.*, *78*, 288–300.
Lee, S. H., and T. E. Whitledge (2005), Primary and new production in the deep Canada Basin during summer 2002, *Polar Biol.*, *28*, 190–197.
Lee, S. H., M. S. Yun, B. K. Kim, H. Joo, S.-H. Kang, C. K. Kang, and T. E. Whitledge (2013), Contribution to total primary production by small phytoplankton in the Chukchi Sea, *Cont. Shelf Res.*, *68*, 43–50.
Lee, Y.-W., M. O. Park, Y.-S. Kim, S.-S. Kim, and C.-K. Kang (2011), Application of photosynthetic pigment analysis using a HPLC and CHEMTAX program to studies of phytoplankton community composition (in Korean with English abstract), *J. Korean Soc. Oceanogr.*, *16*, 117–124.
Lim, J.-H., S. Son, J.-W. Park, J. H. Kwak, C.-K. Kang, Y. B. Son, J.-N. Kwon, and S. H. Lee (2012), Enhanced biological activity by an anticyclonic warm eddy during early spring in the East Sea (Japan Sea) detected by the geostationary ocean color satellite, *Ocean Sci. J.*, *47*, 377–385.
Lozier, M. S., A. C. Dave, J. B. Palter, L. M. Gerber, and R. T. Baber (2011), On the relationship between stratification and primary productivity in the North Atlantic, *Geophys. Res. Lett.*, *38*, L18609, doi:10.1029/2011GL049414.
Mackas, D. L., and A. Tsuda (1999), Mesozooplankton in the eastern and western subarctic Pacific: Community structure, seasonal life histories, and interannual variability, *Prog. Oceanogr.*, *43*, 335–363.
Mackey, M. D., D. J. Mackey, H. W. Higgins, and S. W. Wright (1996), CHEMTAX—A program for estimating class abundances from chemical markers: Application to HPLC measurements of phytoplankton, *Mar. Ecol. Prog. Ser.*, *144*, 265–283.
Malone, T. C. (1980), Algal size, in *The Physiological Ecology of Phytoplankton*, edited by pp. 433–463, Blackwell, Oxford, U. K.
Malone, T. C., and M. B. Chervin (1979), The production and fate of phytoplankton size fractions in the plume of the Hudson River, N.Y. Bight, *Limnol. Oceanogr.*, *24*, 683–696.
Margalef, R. (1978), Life-forms of phytoplankton as survival alternatives in an unstable environment, *Oceanol. Acta*, *1*, 493–509.
Martin, J., J. E. Tremblay, J. Gagnon, G. Tremblay, A. Lapoussière, C. Jose, M. Poulin, M. Gosselin, Y. Gratton, and C. Michel (2010), Prevalence, structure and properties of subsurface chlorophyll maxima in Canadian Arctic waters, *Mar. Ecol. Prog. Ser.*, *412*, 61–84.
Meshcheryakova, I. M. (1960), Seasonal changes of the plankton in offshore waters of the Japan Sea, *Bull. Pacif. Sci. Inst. Fish., Vladivostok.*, *46*, 95–144.
Min, D.-H., and M. J. Warner (2005), Basin-wide circulation and ventilation study in the East Sea (Sea of Japan) using chlorofluorocarbon tracers, *Deep Sea Res., Part II*, *52*, 1580–1616.
Nishioka, J., S. Takeda, I. Kudo, D. Tsumune, T. Yoshimura, K. Kuma, and A. Tsuda (2003), Size-fractionated iron distribution and iron-limiting processes in the subarctic NW Pacific, *Geophys. Res. Lett.*, *30*(14), 1730, doi:10.1029/2002GLO16853.
Parsons, T. R., Y. Maita, and C. M. Lalli (1984), *A Manual of Chemical and Biological Methods for Seawater and Analysis*, 173 pp., Pergamon, Oxford.
Piontkovski, S. A., R. Williams, and T. A. Melnik (1995), Spatial heterogeneity, biomass and size structure of plankton of Indian Ocean: Some general trends, *Mar. Ecol. Prog. Ser.*, *117*, 219–227.
Poole, H. H., and W. R. G. Atkins (1929), Photo-electric measurements of submarine illumination throughout the year, *J. Mar. Biol. Assoc.*, *16*, 297–324.
Rebstock, G. A., and Y. S. Kang (2003), A comparison of three marine systems surrounding the Korean peninsula: Response to climate change, *Prog. Oceanogr.*, *59*, 357–379.

Rho, T. K., T. Lee, G. Kim, K.-I. Chang, T. H. Na, and K.-R. Kim (2012), Prevailing subsurface chlorophyll maximum (SCM) layer in the East Sea and its relation to the physic-chemical properties of water mass, *Ocean Polar Res.*, *34*, 413–430.

Riser, S. C., and G. Jacobs (2005), The Japan/East Sea: A historical and scientific introduction, *Deep Sea Res., Part II*, *52*, 1359–1362.

Shiomoto, A. (2000), Efficiency of water-column light utilization in the subarctic northwestern Pacific, *Limnol. Oceanogr.*, *45*, 982–987.

Sundbäck, K., and P. Snoeijis (1991), Effects of nutrient enrichment on microalgal community composition in a coastal shallow-water sediment system: An experimental study, *Bot. Mar.*, *34*, 341–358.

Talley, L. D., D.-H. Min, V. B. Lobanov, V. A. Luchin, V. I. Ponomarev, A. N. Salyuk, A. Y. Shcherbina, P. Y. Tishchenko, and I. Zhabin (2006), Japan/East Sea water masses and their relation to the sea's circulation, *Oceanography*, *19*, 32–49.

Wright, S. W., and R. L. van den Enden (2000), Phytoplankton community structure and stocks in the Eastern Antarctic marginal ice zone (BROKE survey, January–March 1996) determined by CHEMTAX analysis of HPLC pigment signatures, *Deep Sea Res., Part II*, *47*, 2363–2400.

Yamada, K., J. Ishizaka, and H. Nagata (2005), Spatial and temporal variability of satellite primary production in the Japan Sea from 1998 to 2002, *J. Oceanogr.*, 857–869.

Yamamura, O., S. Honda, O. Shida, and T. Hamatsu (2002), Diets of walleye pollock Theragra chalcogramma in the Doto area, northern Japan: Ontogenetic and seasonal variations, *Mar. Ecol. Prog. Ser.*, *238*, 187–198.

Yoo, S., and J. Park (2009), Why is the southwest the most productive region of the East Sea/Sea of Japan?, *J. Mar. Syst.*, *78*, 301–315.

Zapata, M., F. Rodriguez, and J. L. Garrido (2000), Separation of chlorophylls and carotenoids from marine phytoplankton: A new HPLC method using a reversed phase C_8 column and pyridine-containing mobile phases, *Mar. Ecol. Prog. Ser.*, *195*, 29–45.

Zhang, C. I., and Y. Gong (2005), Effect of ocean climate changes on the Korean stock of Pacific saury, *Cololabis saira* (BREVOORT), *J. Oceanogr.*, *61*, 313–325.